STATE OF THE CLIMATE IN 2014

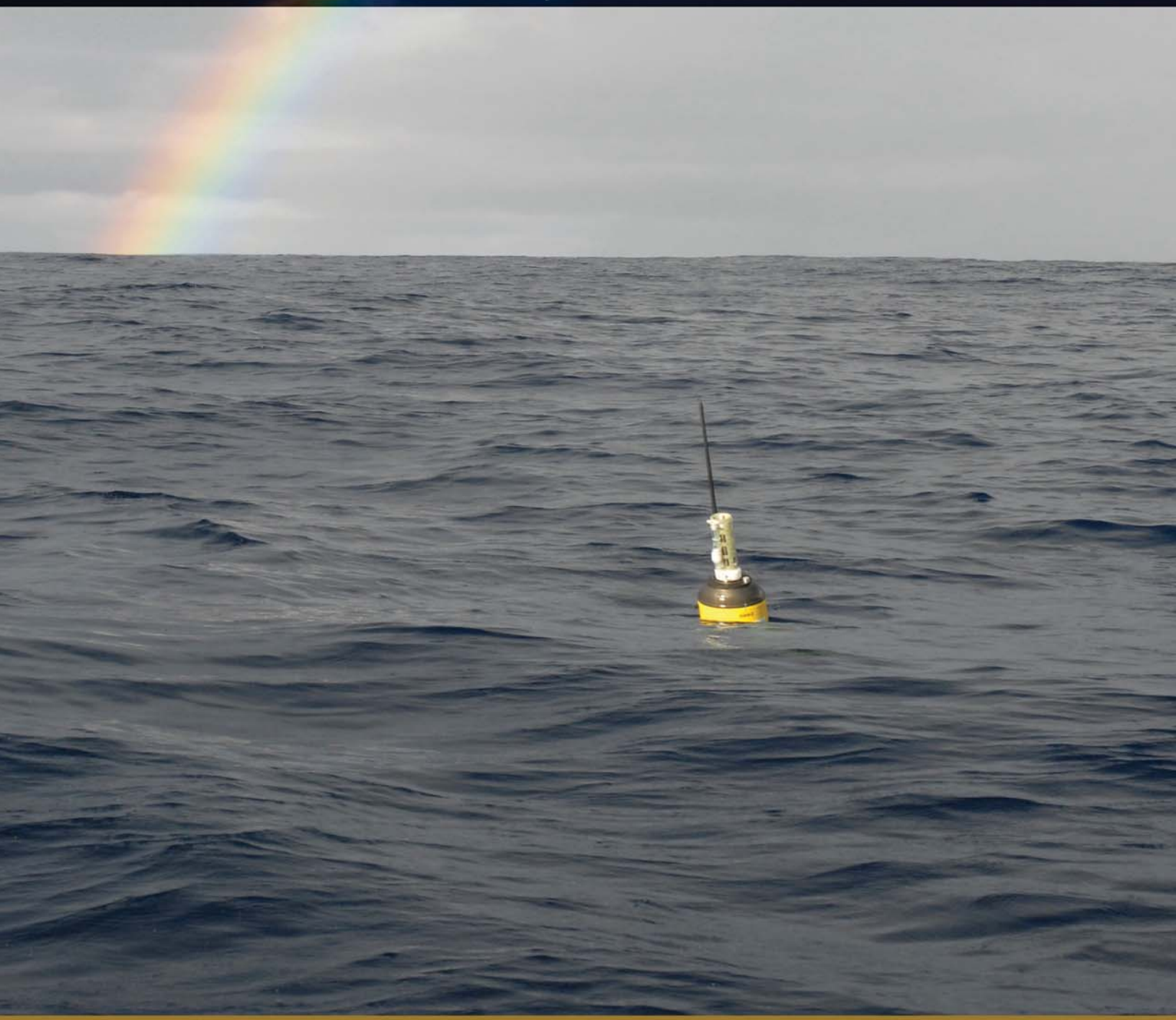

Special Supplement to the
Bulletin of the American Meteorological Society
Vol. 96, No. 7, July 2015

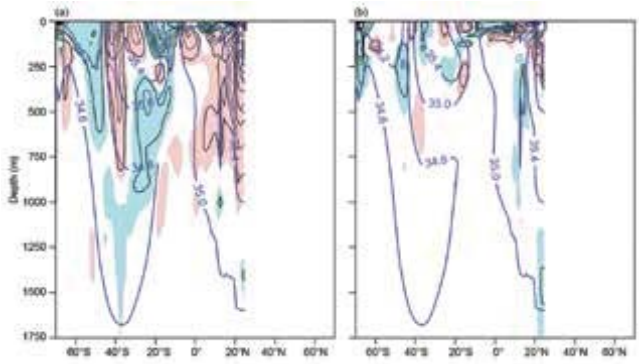

Fig. 3.16. Zonally averaged (a) 2014 salinity anomaly and (b) 2014 minus 2013 salinity field for the Indian Ocean. Details follow Fig. 3.14.

at latitudes north of 30°S covered most of the basin from Australia to Africa, a westward expansion that occurred over the last three years (Boyer et al. 2014). South of 30°S, the salty anomaly extended across the entire basin in a narrow band north of 50°S, a continuation of the pattern of 2013. The salinity change from 2013 to 2014 in the south Indian Ocean was small (<0.02; Fig. 3.16b), except south of 60°S where the data coverage is coarse, and in the upper 50 m near the equator. Most of the north Indian Ocean anomalies for 2014 continued to be salty to depths exceeding 700 m. From 2013 to 2014, changes in the north Indian Ocean were mainly confined to the upper 150 m, with a freshening in the upper 100 m within 5° of the equator and increasing salinity in the subtropics near the surface, which continued in the 50–150 m layer toward the equator.

g. Surface currents—K. Dohan, G. Goni, and R. Lumpkin

This section describes ocean surface current variability, emphasizing tropical events, western boundary currents, transports derived from ocean surface currents, and features such as rings (large eddies) inferred from surface currents. Global surface currents (Fig. 3.17) are obtained from satellite (sea surface height, wind stress, and SST) and in situ (global array of drogued drifters and moorings) observations and discussed by individual basin below. Current variability can also be derived from sources such as shipboard current measurements, expendable bathythermograph repeat sections, and underwater glider data. The strongest, most persistent anomaly in global surface currents in 2014 was the stronger-than-normal eastward flow of the Pacific North Equatorial Countercurrent (NECC). In addition, in the North Pacific, the Kuroshio and its extension remain about 1° north of their climatological positions in 2014.

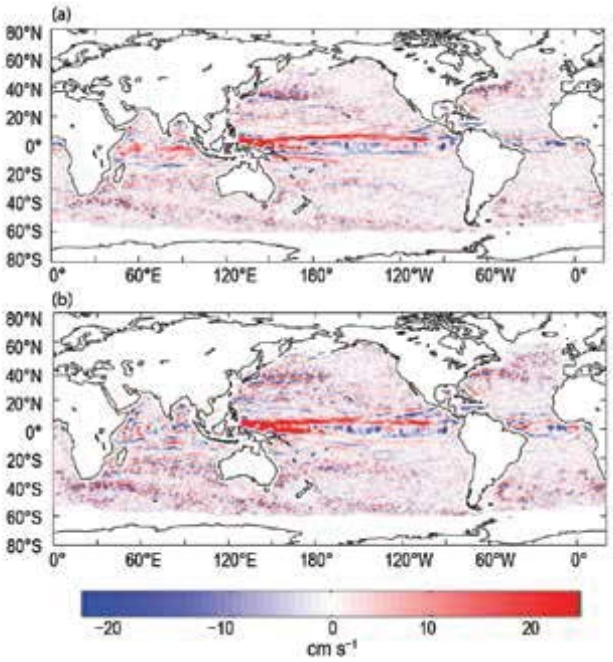

Fig. 3.17. Global zonal geostrophic surface current anomalies relative to 1993–2007 for (a) 2014 and (b) 2014–2013 (cm s^{-1}), based on OSCAR currents derived from altimetry, ocean vector winds, and SST (Bonjean and Lagerloef 2002; Dohan and Maximenko 2010).

1) Pacific Ocean

January 2014 began with a strengthening of climatological conditions. Westward anomalies of ~20 cm s^{-1} were present in the equatorial Pacific between 170° and 100°W. Farther east and north, between 160° and 120°W and at 7°N, eastward anomalies of ~20 cm s^{-1} indicated a strengthening of the NECC. This strengthening occurred throughout 2014 (Fig. 3.17), changing with the seasonal position, with monthly anomalies generally between 10 and 30 cm s^{-1}. February saw a dramatic change in equatorial currents. Eastward anomalies developed between 140°E and 150°W along the equator, ranging from 70 cm s^{-1} in the west to 40 cm s^{-1} in the east, and peaking above 1 m s^{-1} at 170°E. Westward anomalies of ~30 cm s^{-1} persisted along the equator east of 110°W. By March, eastward anomalies spanned the entire basin with some regions reaching over 1 m s^{-1}. These anomalies lessened some in April and May. June saw a complete reversal of the equatorial anomalies with strong westward anomalies present across the basin, ranging between 20 and 80 cm s^{-1}, strongest in the center of the basin, reaching a peak at 150°W. This continued through July, shifting to the east with anomalies of 50 cm s^{-1} between the dateline and 100°W, and then subsided in August. Some westward anomalies of ~10 cm s^{-1} were beginning to appear in December, west of 140°W.

The annual average zonal current anomaly for 2014 in the Pacific (Fig. 3.17a) was dominated by the persistent strengthening of the NECC. Along the equator, although both eastward and westward anomalies were present at different times of the year, the predominant anomalies in the annual mean were eastward in the western part of the basin and westward in the central. This pattern is reflected in the 2014–2013 map (Fig. 3.17b) since mean currents for 2013 were near the 1993–2007 climatology.

Surface current anomalies in the equatorial Pacific typically lead SST anomalies by several months (cf. Lagerloef et al. 2003). In addition, warm SST anomalies reach their maximum at the point of reversal of eastward anomalies. This leading nature can be seen in the first principal empirical orthogonal function (EOF) of zonal surface current (SC) anomaly and separately of SST anomaly in the tropical Pacific basin (Fig. 3.18). The year 2014 began with a strong indication of an El Niño event, with the SC EOF reaching more than 2 standard deviations in amplitude. The SST EOF amplitude can be seen to rise at the beginning of the year until the point at which SC anomalies reversed as described above (marked by the zero-crossing of the SC EOF) and halted the advection process, resulting in an ENSO-neutral 2014.

The Kuroshio remains approximately 1° latitude north of its climatological position, holding there since 2010. This shift is evident in the alternating zonal bands of ~40 cm s^{-1} anomalies at 33°–36°N, 140°–160°E. The maximum northern extent of the Kuroshio, where it separates from the continent, shifted slightly south from 37°N in 2013 down to 36.3°N in 2014. Meanders and shifts of the western boundary currents such as this dominate the 2014–2013 map (Fig. 3.17b) outside of the tropics.

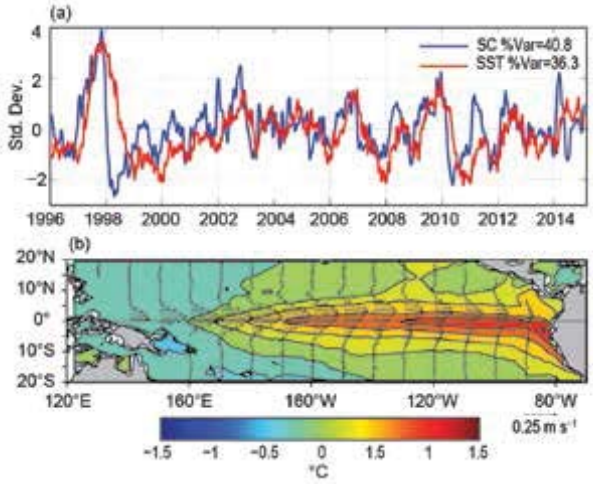

Fig. 3.18. Principal empirical orthogonal functions (EOFs) of surface current (SC) and SST anomaly variations in the tropical Pacific from the OSCAR model. (a) Amplitude time series of the EOFs normalized by their respective standard deviations. (b) Spatial structures of the EOFs.

2) Indian Ocean

In the western equatorial Indian Ocean, the year began with ~10 cm s^{-1} eastward anomalies over the region 2°S–2°N, 40°–70°E. These anomalies were removed in February by the westward equatorial currents that developed during the northeast monsoon season (cf. Beal et al. 2013), although a strong eastward anomaly of ~60 cm s^{-1} persisted in the westernmost equatorial region. By March, only westward anomalies of ~20 cm s^{-1} remained between 4°S and 4°N. Zonal bands of eastward anomalies from 10 to 50 cm s^{-1} developed in this region between 8°S and 2°N starting in May and carrying through until December, typically spanning about 3° latitude. The location and intensity of the band of eastward anomalies shifted throughout the year, from a center around 1°S in May to 5°S in September, and separating into two bands around 0° and 5°S during October–December. Typical anomaly values were between 10 and 20 cm s^{-1}. December showed strong eastward anomalies ~50 cm s^{-1} in the center of the basin. A band of westward anomalies ~20 cm s^{-1} along the equator in August and September was coincident with the shift south of eastward anomalies.

Values for the altimetry-derived annual mean transport of the Agulhas Current showed a decreasing trend in transport throughout 2014 with a mean of 53 Sv, compared to a mean of 56 Sv in 2013, but only 46 Sv in 2012 (Lumpkin et al. 2014). The 2014 transport value of 51 Sv was still above the climatological value, with positive transport anomalies for all months in 2014 except December.

3) Atlantic Ocean

In the tropical Atlantic, the year began with westward anomalies of ~15 cm s^{-1} along the equator east of 20°W. Starting in February, the currents returned to near climatological values until April, when eastward anomalies of ~20 cm s^{-1} arose in both the equatorial flow west of 20°W and the flow at 3°S east of 20°W. Eastward anomalies continued to appear, although to a lesser degree, throughout the basin between 3°S and 4°N through May. An intensification of the climatological flow began in June: along 2°N there was increased westward flow of ~30 cm s^{-1} between 30°W and 0° and an increased eastward flow between 40° and 35°W. The westward flow increased in July, with westward anomaly zonal bands of 15 and 25 cm s^{-1} centered along 4°S and 2°N, respectively. July also saw

an intensification of the NECC eastward zonal band along 6°N between 40° and 20°W of 10 cm s^{-1}. These off-equatorial anomalies decreased during August, although westward anomalies persisted between 0° and 3°N. The currents remained close to climatology until December, when an intensification of the NECC at 6°N began again between 50° and 40°W with eastward anomalies over 40 cm s^{-1}.

The shedding of rings by the North Brazil Current (NBC) is a pathway for Southern Hemisphere water into the North Atlantic basin. Sea surface height anomalies along the NBC ring corridor exhibited lower values in 2014 than during 2010–11, but average values with respect to the 1993–2010 mean (www.aoml.noaa.gov/phod/altimetry/cvar/nbc). The NBC shed six rings during 2014, which is average in the region. The largest sea surface height anomalies found in this region during the second half of 2014 represent larger-than-average rings shed by the NBC.

The Yucatan Current, the component of the North Atlantic surface circulation that flows through the Yucatan Straits, exhibited larger-than-average values (>3 Sv) during 2012 and 2013, and decreased to average values during 2014 (Fig. 3.19). The variability of this transport is of importance since the Florida Current transport variability, an indicator of the strength of the Atlantic meridional overturning circulation (section 3h), approximately follows the variability of the Yucatan Current.

Farther north in the Atlantic, the mean position of the Gulf Stream along the coast between 35.5° and 38°N sharpened and shifted 1° northward from 2013 to 2014. This is a slightly smaller shift north from the 1993–2007 mean for 2014, as 2013 was slightly shifted south of climatology. The mean position of the Loop Current extended fully into the Gulf of Mexico in 2014, in contrast to 2013 where the mean position only partly entered the Gulf.

In the southwest Atlantic Ocean, the separation of the Confluence Front from the continental shelf break continued to exhibit annual periodicity driven by wind stress curl variations (cf. Goni and Wainer 2001). The annual mean position of the front in 2014 was close to its climatological mean for the altimetric time period 1993–present (cf. Lumpkin and Garzoli 2010; Goni et al. 2011).

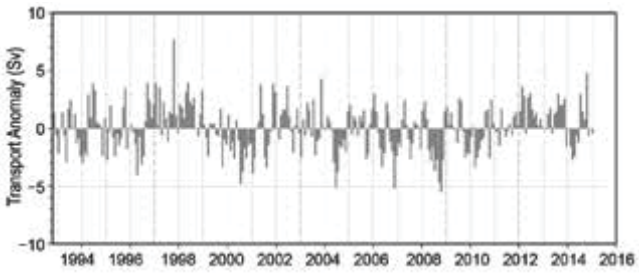

Fig. 3.19. Transport of the Yucatan Current estimated using a combination of sea surface height anomalies and climatological hydrography.

h. Meridional overturning circulation observations in the North Atlantic Ocean—M. O. Baringer, G. McCarthy, J. Willis, D. A. Smeed, D. Rayner, W. E. Johns, C. S. Meinen, M. Lankhorst, U. Send, S. A. Cunningham, and T. O. Kanzow

Within the large-scale ocean circulation known as the meridional overturning circulation (MOC) surface waters at high latitudes cool, become denser, sink, and return to lower latitudes. This circulation—identified as overturning because surface waters are transformed into deep and bottom waters and meridional in that waters are transported north and south, redistributing heat, fresh water, carbon, and nutrients—represents an important mechanism for how the ocean regulates climate. Previous *State of the Climate* reports (e.g., Baringer et al. 2013) and reviews (e.g., Macdonald and Baringer 2013; Lozier 2012; Srokosz et al. 2012) discuss the importance of the MOC and its impact on climate variability and ecosystems. This section reports the recent results provided by three time-series MOC observing systems in the North Atlantic at 16°N, 26°N, and 41°N.

The longest time series of ocean transport to serve as an index of the MOC's strength in the North Atlantic (e.g., Duchez et al. 2014) is from the Florida Current (FC, as the Gulf Stream is called around 26°N), which has been measured since 1982. Measurements continue through 2014 and beyond, with two brief gaps in the time series during 1–3 January 2014 and 8–13 March 2014. The median 1982–2014 transport of the FC is 31.9 ± 0.26 Sv (one standard error of the mean based on an integral time scale of about 20 days) with a small downward trend of −0.31 ± 0.27 Sv $decade^{-1}$ (errors using 95% significance with a decorrelation time scale of about 20 days; Fig. 3.20). In 2014 the annual median was 30.5 ± 1.2 Sv, the third lowest since 1982. The daily FC transport values as compared to all previous years (Fig. 3.20) indicate that 2014, like 2013, had several unusually low transport anomalies (extremes defined as outside the 95% confidence limits for daily values) during 8 January, 18 April–5 May, 26–29 August, and 9–11 December 2014. The lowest transport observed occured on 2 May, reaching 20.7 Sv. Transports less than 23 Sv persisted for a 5-day period centered on this date. This value is the 18th lowest transport recorded since 1982. During 2014 there were no high transport events that exceed the 95% confidence limits; the highest transport was 37.9 Sv on 15 October.